



Physical properties and biological activity of methyldopa drug carrier cellulose derivatives: Theoretical study



CrossMark

Mudeer Mubarak M^a, Fadhela M Hussein^a, Ramzie R.AL-ani1^{a*}

^a Department of Chemistry, College of Science, Mustansiriyah University

Abstract

The complete computational study of the methyldopa drug and its derivatives prodrug 1-4(methyldopa-cellulose (Ce), methyldopa-carboxymethyl cellulose(CMC), methyldopa-maleic anhydride cellulose (MAC)and methyldopa-hydroxypropyl cellulose(HPC)) was performed by Density Function theory method with the Becker's three parameter hybrid functional (B3LYP) functional and 6-31G++ (d, p) basis set using Gaussian 09 program. The Density Function theory (DFT) DFT method is used to calculate the optimal molecular structure, vibrational spectra, highest occupied molecular orbital energies (HOMO), lowest unoccupied molecular orbital energies (LUMO), electronic properties (total energy, dipole moment, electronegativity, chemical hardness and softness), biological activity, and molecular surfaces. Using the reaction coordinate method to quantify the energy enthalpy and activation energy of O-R bond rupture. The result shows the derivatives that are hoped to have preference in their use as carriers are (methyldopa-Ce) and (methyldopa-MAC), which gave the drug acid as a product of the O-R bond breaking process in an irreversible reaction.

© 2020 NIODC. All rights reserved

Keywords: Cellulose, methyldopa, DFT, HOMO-LUMO, PM3, Biological Activity;

1. Introduction

Hypertension is related to an elevated risk of stroke, myocardial infarction, and heart problems. Methyldopa is a centrally functioning antihypertensive agent that was widely used to regulate blood pressure in the 1970s and 80s. At present, its use replaced by groups of antihypertensive medications with lower side effects, but because of its reduced cost, it is still used in developed countries [1],[2]. An analysis of its relative efficacy with respect to surrogate and therapeutic results compared with placebo is justified [1]. Chemically, known as (3-hydroxy- α -methyl-L-tyrosine) (Fig. 1). The pharmaceutical company produces and sources new drug delivery formulas, compounds, sells and dispenses them. The primary target is to accomplish provide innovative and reliable

cost-effective, safe and non-toxic drug delivery approaches. Similar biopolymers can be exploited for drug use procedures for precise location drug delivery [3]. Cellulose has been used in formulations for medications along with its derivative components for decades and its application is most widely stated to be a viscosity improver in topical formulations, releasing agents in oral formulations [4]. Cellulosic for various medicinal uses are biocompatible, reproducible and recyclable. Typical cellulosic medicine Methyl cellulose, ethyl cellulose, hydroxymethyl cellulose, hydroxyl propyl cellulose, and carboxymethyl cellulose are included [5]. In scope of this research, cellulose and its derivatives were used carboxymethyl cellulose (CMC), hydroxyl propyl cellulose (HPC) and maleic anhydride cellulose (MAC) for a drug carrier (Fig. 1). The main aim of this research was to develop new methyldopa prodrugs for the treatment of high

*Corresponding author e-mail: mudeer_sm@yahoo.com;

Receive Date: 14 March 2021, Revise Date: 05 April 2021, Accept Date: 08 April 2021

DOI: 10.21608/EJCHEM.2021.67857.3479

©2021 National Information and Documentation Center (NIDOC)

blood pressure that have a higher bioavailability than the current drug and the potential to release their parent drugs in a safe and side-effect-free manner, using theoretical research and a variety of orbital and molecular mechanics methods.

2. EXPERIMENTAL

2.1. Computational methods

The quantum simulations were carried out using the Gaussian-09 software package and Gaussian View 06 kit, which included full geometry optimizations. [6]. The geometry optimization was carried out for methyl dopa as standards and cellulose derivatives as suggested carriers D (1–4), (Figure-1). Using the (6-31G++/d,p) level ab-initio (DFT) Density Function theory method [7]. The system of parameterized model number 3 (PM3) semi-empirical and open-shell (UHF/STO-3G) was used for evaluating the reaction path of the breakup of (R-O) bonds. The biological activity was calculated in aqueous medium of the studied prodrugs. The DFT method has been studied for certain quantum chemical parameters in vacuum for non-linear optical (NLO) properties of associated prodrugs [8]. These quantum chemical descriptors include energy of a highest occupied orbital molecules (HOMO), energy of a lowest occupied orbital molecules (LUMO), energy of ionization (IE), affinity of electrons (EA), energy gap (Egap), absolute hardness (η), absolute softness (S), electronegativity (χ), chemical potential (CP), electrophilicity index (ω), additional electronic charges (Nmax), Polarizability (α), Polarizability Urea was used as a reference in the calculations for determining NLO properties [9]. The quantum chemical descriptors (QCDs) were calculate using Equations(1–10) [10][11].

$$I_p (\text{Ionization potential}) = -E_{\text{HOMO}} \quad (1)$$

$$EA (\text{Electron affinity}) = -E_{\text{LUMO}} \quad (2)$$

$$E_{\text{gap}} = E_{\text{LUMO}} - E_{\text{HOMO}} \quad (3)$$

$$\eta (\text{hardness}) = (I_p - EA) / 2 \quad (4)$$

$$S (\text{global softness}) = 1 / \eta \quad (5)$$

$$X (\text{electronegativity}) = (I_p + EA) / 2 \quad (6)$$

$$\omega (\text{electrophilicity}) = -\chi^2 / 2\eta = \mu^2 / 2\eta \quad (7)$$

$$CP (\text{chemical potential}) = -\chi \quad (8)$$

$$N_{\text{max}} = -CP / \eta \quad (9)$$

$$\alpha (\text{Polarizability}) = 1/3(\alpha_{xx} + \alpha_{yy} + \alpha_{zz}) \quad (10)$$

$$\beta_o (\text{hyperpolarizability}) = [(\beta_{xxx} + \beta_{xyy} + \beta_{xzz})^2 + (\beta_{yyy} + \beta_{yzz} + \beta_{yxx})^2 + (\beta_{zzz} + \beta_{zxx} + \beta_{zyy})^2]^{1/2}$$

3. RESULTS AND DISCUSSION:

3.1. Study of structures for geometrical optimization

The initial geometry was optimized using standard geometrical parameters, and the equilibrium geometry was calculated using energy minimization. Figure 1 depicts the molecule's optimized ground state structure.

The optimized structure of the drug methyl dopa was compared with prodrug and its four derivatives using (DFT/B3LYP/6-31G++ d,p). The bond lengths of the drug acid (R = -H) were calculated and the bond length was O-H (0.97245 Å), the lengths of the bonds of unprepared ester derivatives were also extracted practically in the equilibrium geometric form. The focus has been on the length of the O-R group that connects the ester group in the drug part with the group carrying it in these derivatives, which was found to be ranged in length (1.3522 -1.5043 Å) Table(1) . It was also found that the shorter length of the O-R is due to the derivative (MAC) because maleic anhydride has two carbonyl groups. The energy of EHOMO, and the energy of the ELUMO, and the energy difference between them, $\Delta E(\text{HOMO-LUMO})$, were calculate and compared, which ranged between (4.6135-5.6222 eV). The methyl dopa-CMC as prodrug has less value energy gap (4.6135 eV) implies that show high chemical reactivity (less stable) [12]. As for the dipole moment, it ranged between (3.5612-18.3518 Debye) and the highest value of the derivative prodrug (MAC) compared to the original drug, this indicates that the more valuable derivative is more polar and therefore faster decomposition.

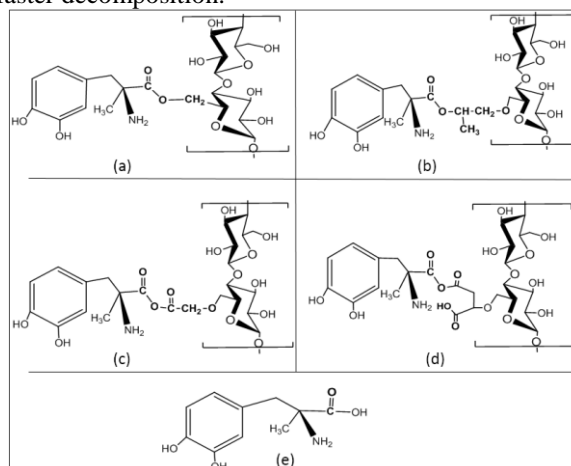


Figure 1: Structure of methyl dopa prodrugs R= a- Cellulose(CE), (b)- Hydroxypropyl cellulose(HPC) , (c)-Carboxymethyl cellulose(CMC), (d)-Maleic anhydride cellulose(MAC) and (e) methyl dopa.

3.2. Frontier molecular orbitals

The molecular frontier orbitals will provide reasonable quality predictions of excitement properties and the ability to transport electron [29, 30]. The lowest unoccupied molecular orbital (LUMO) has a lower energy and is deficient in electrons, while the highest occupied molecular orbital (HOMO) has a higher energy and is abundant in electrons, and thus has a strong electron donating potential, and is often referred to as frontier molecular orbitals (FMOs) [15]. The

LUMO and HOMO plots in 3D are shown. As seen in Figure 3.

3.3. Molecular Electrostatic Potential Surface

Electrostatic surface molecular potential (MEP) is a useful descriptor for determining where electrophilic attack and nucleophilic reactions occur, as well as studying biological recognition processes. MEP at the B3LYP/6-311++G (d, p) optimized geometry was determined to predict electrophilic and nucleophilic attack reactive sites for the investigated molecule. The chemically active sites and comparative reactivity of atoms are depicted in Figure (4). The potential value increases in the order red < orange < yellow < green < blue. The electrophilic reactivity was associated with the negative (red and yellow) regions of MEP, while nucleophilic reactivity was associated with the positive (blue) regions. [16]. The green colour scheme represents a potential split between the two extreme regions of red and blue. Out of Fig(4), it is clear that for the title compound, the more electronegative region (electrophilic) region is over the electronegative O atoms, while the more electropositive region (nucleophilic) region is over all of the OH groups' H atoms.

3.4. Quantum Calculation for O-R Bond Rupture Energy

Using the co-ordinate reaction method after balancing [17], enthalpy changes have been controlled by gradually increasing the distance between the two atoms. This approach restricts one bond long to the required degree of freedom while freely optimizing all other variables. Table (2) and (3) shows the final results of the (O-R) breaking energies calculated according to the PM3 and UHF calculation method of methyl dopa ester derivatives. Figure 5 (1-4) shows the energy curves for breaking the O-R bundle of methyl dopa derivatives. As for values the energy of the products of thermal cracking of the derivatives, the energy of the transition state, the activation energy and the nature of the products, they differed according to the nature of the group carrying the drug part (O-R).

The derivatives that are hoped to have preference in their use as carriers are (methyl dopa-cellulose) and (methyl dopa-MAC), which gave the drug acid as a product of the O-R bond breaking process in an irreversible reaction figure 6. The cracking heat ΔH_c and ΔE_{tot} (cracking) of the prodrug (methyl dopa-cellulose) was positive and endothermic (29.176

kcal/mol) and (52.136 kcal/mol) by PM3 and ab initio HF respectively, and the activation energy were (78.843 and 103.001 kcal/mol). While prodrug (methyl dopa-MAC) the cracking heat ΔH_c and ΔE_{tot} (cracking) was negative and exothermic (-3.256 and -7.243 kcal/mol) that show in figure 5.3. In the case of (methyl dopa-MAC) a proton transition occurs from an atom (H81) at the bond length (2.504 Å) from the carboxyl group of maleic anhydride to the carboxyl group of the separate drug and the formation of hydrogen bonds and then the separation of cellulose maleic anhydride figure (8.3.).

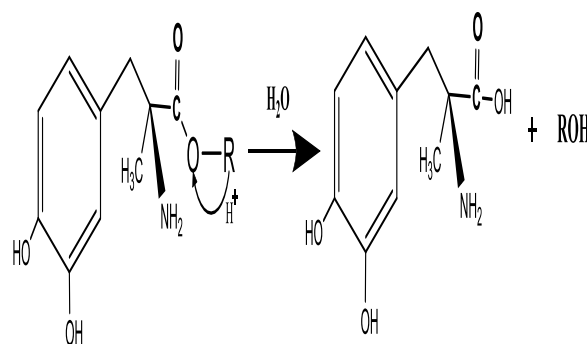


Fig. 6: The products of the calculated O-R bond rupture reaction in methyl dopa (cellulose, MAC) ester prodrugs.

The suggested prodrugs of drugs carriers (methyl dopa-CMC, methyl dopa-HPC) in (figure 8.2,8.4) were product cation and anion for (O-R) rupture process in an irreversible reaction Figure7, with ΔH_c and ΔE (endothermic reaction) ranging from (36.87 to 45.62 kcal/mol) or from (63.59 to 65.31 kcal/mol) for PM3 and HF respectively. The activation energy is from (74.11 to 57.25 kcal/mol) or from (127.94 to 93.13 kcal/mol) for PM3 and HF respectively Tables (2, 3).

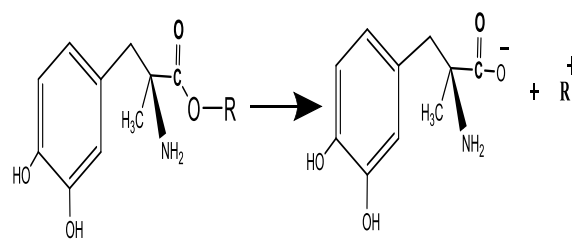


Fig.7: The products of the calculated O-R bond rupture reaction in methyl dopa (CMC, HPC) ester prodrugs.

3.5. Vibrational Analysis

The vibrational analysis of methyl dopa drug and its four prodrug derivatives are performed on the basis of the characteristic vibrations. The observed and calculated frequencies (cm⁻¹) using DFT (6-31G++ d, p) were illustrate in Table (4). Show the calculated IR intensities and frequencies were compared with the

experimentally [18] only methyldopa drug obtained data due to other derivatives not experimentally studied yet figure (9). Any bands were not detected in the experimental spectrum in computed IR spectrums. Since the measured vibrational frequencies were solvent and steric, the experimental results showed strong concordance with the results. The carbon-carbon stretching modes of the phenyl group are expected in the range from 1400 to 1650 cm⁻¹ [19], in theoretical calculate by DFT found the Benzene has two degenerate modes at (1557-1680 cm⁻¹) and the frequency of the NH within the amine group NH₂ was found to range between (3492- 3560 cm⁻¹). While the frequency of C=O belonging to ester and anhydride

groups range between (1654-1795 cm⁻¹). Whereas the frequency of the (C-O-C) strain that connects the ester group in the drug part with the carrier group is important and we note that the derivative, which is not expected to be used as a prodrug, has a high frequency value, so that the force constant is large and difficult to break and thus does not give the drug acid as in methyldopa-CMC and methyldopa-HPC, and this corresponds to the results of Break the (R-O) previously mentioned. In general, greater values of frequencies refer to the largest bond force constant of these bonds, and the lowest value refers to the lowest force constant [20].

Table 1: DFT / 6-31G++ (d, p) calculations for some physical properties of the methyldopa and derivatives at the minimize equilibrium geometries.

| Property | METHYLDOP A -H | METHYLDOP A - CELLULOSE | METHYLDOP A - C M C | METHYLDOP A - M A C | METHYLDOP A -HPC |
|-----------------------|----------------------|-------------------------------|------------------------|------------------------|---------------------|
| E total (a.u) | -744.6087 | -1965.4083 | -2193.2291 | -2421.0934 | -2158.5677 |
| HOMO(ev) | -6.02608 | -5.84676 | -5.96186 | -5.99669 | -5.88912 |
| LUMO(ev) | -0.65468 | -0.22448 | -1.34829 | -1.00788 | -0.72598 |
| Eg(ΔE)ev | 5.37140 | 5.62227 | 4.61357 | 4.98881 | 5.16323 |
| D.M (debye) | 3.56128 | 4.032354 | 11.56338 | 18.35184 | 9.51831 |
| Bond(O-R)ester | 0.97245 | 1.47836 | 1.40256 | 1.35220 | 1.50432 |

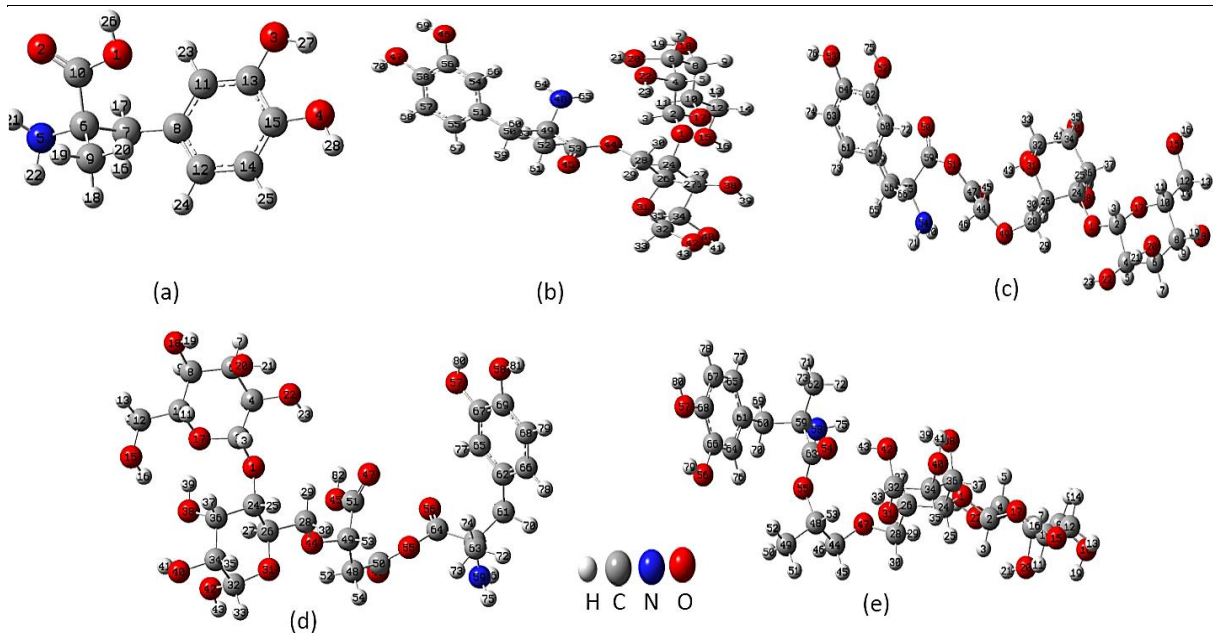


Fig. 2 : Geometry optimizations structure of Methyldopa and derivatives prodrug calculated by DFT/ 6-31G++(d,p) method (a)methyldopa, (b)methyldopa- cellulose.(c) methyldopa-CMC.(d) methyldopa-MAC.(e)methyldopa—HPC.

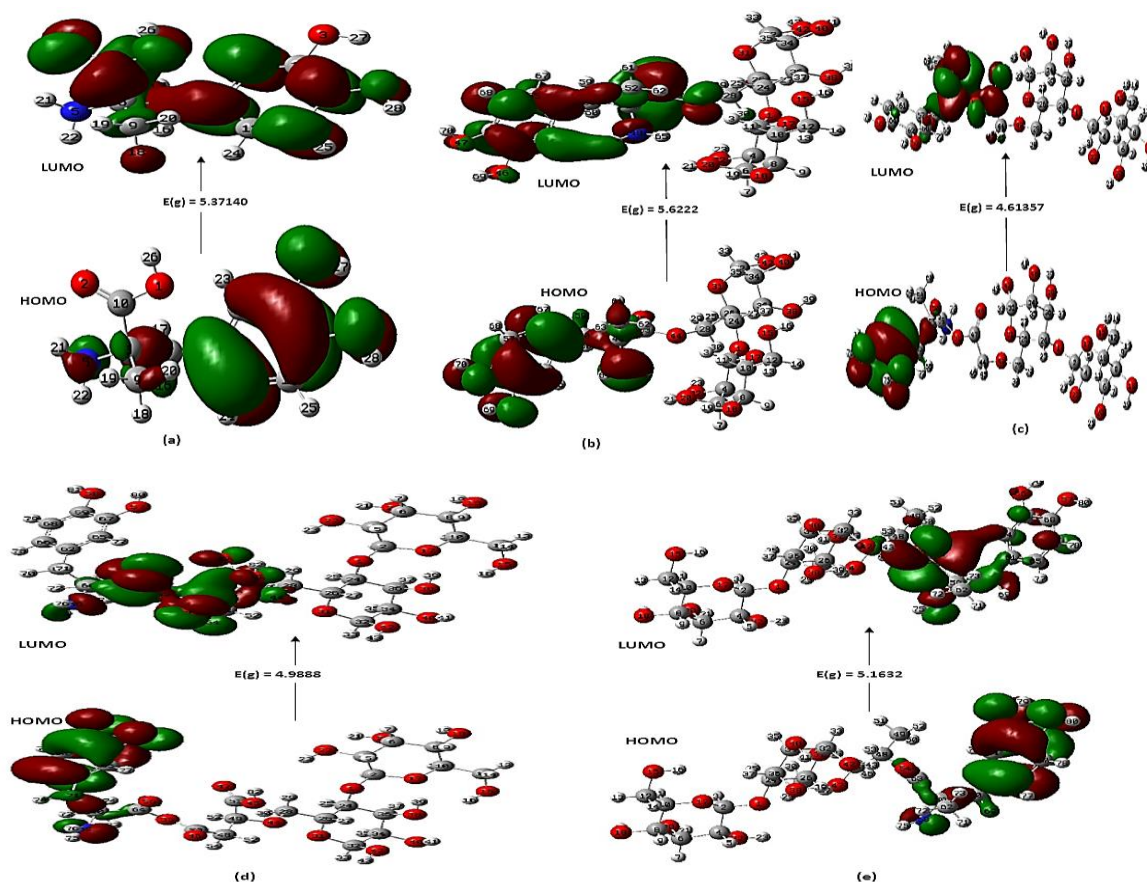


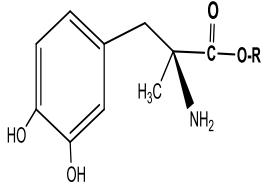
Fig. 3: The frontier molecule orbital (HOMO and LUMO) of (a) methyldopa, (b) methyldopa-cellulose, (c) methyldopa-CMC, (d) methyldopa-MAC, (e) methyldopa-HPC.

Table 2: HF calculated energies values for the O-R bond breakage reactions in methyldopa derivatives cellulose suggested as carriers.

| Methyldopa Prodrug | -R | E _{total} Reactant (Kcal/mol) | E _{total} Product (Kcal/mol) | ΔE _c (Kcal/mol) | E _{a#} (Kcal/mol) | E _{t.s} (Kcal/mol) |
|--------------------|------------|--|---------------------------------------|----------------------------|----------------------------|-----------------------------|
| | -Cellulose | -1210898.58 | -1210846.44 | 52.1360 | 103.001 | -1210795.58 |
| | -CMC | -1351259.88 | -1351194.55 | 65.31883 | 127.9403 | -1351131.93 |
| | -MAC | -1491615.54 | -1491622.79 | -7.243232 | 61.6895 | -1491553.85 |
| | -HPC | -1329881.85 | -1329818.25 | 63.594610 | 93.1398 | -1329788.71 |

* ΔE_{total} (cracking) = E_{total} (product) - E_{total} (reactant), E_{a#} = E_{total} (transition) - E_{total} (reactant)

Table 3: PM3 calculated energies values for the O-R bond rupture reactions in Methyldopa derivatives cellulose suggested as carriers.

| Methyldopa Prodrug | -R | ΔH_f Reactant (Kcal/mol) | ΔH_f Product (Kcal/mol) | ΔH_c (Kcal/mol) | $E_a^\#$ (Kcal/mol) | $E_{t,s}$ (Kcal/mol) |
|---|------------|--|---------------------------------------|----------------------------|------------------------|-------------------------|
|  | -Cellulose | -582.1882 | -553.0126 | 29.176 | 78.8439 | -503.3440 |
| | -CMC | -666.03791 | -620.40925 | 45.62866 | 74.1177 | -591.9201 |
| | -MAC | -762.62145 | -765.87818 | -3.256725 | 52.317812 | -710.3036 |
| | -HPC | -642.78464 | -605.91023 | -605.9102 | 57.259375 | -585.5252 |

* ΔH (cracking) = ΔH (product) - ΔH (reactant), $E_a^\# = \Delta H$ (transition state) - ΔH (reactant)

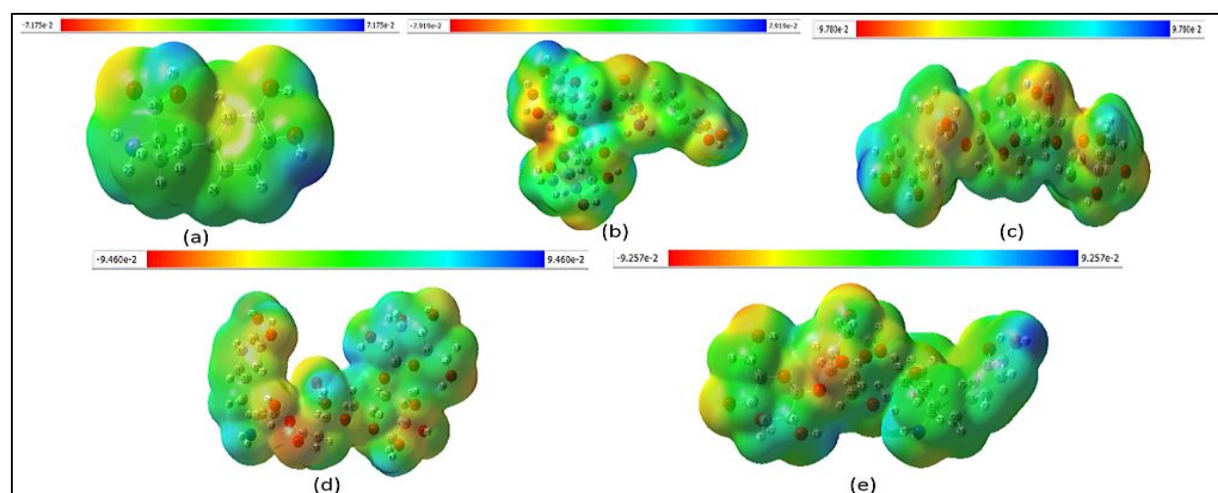


Fig. 4: Molecular electrostatic potential map of (a) methyldopa, (b) methyldopa-Cellulose, (c) methyldopa-CMC, (d) methyldopa-MAC, (e) methyldopa-HPC.

Table 5 : Quantum chemical descriptors of the biological reactivity calculated by DFT/B3LYP/ (6-31G)++(d,p) in aqueous solution.

| Property | METHYLDOPA | METHYLDOPA-CELLULOSE | METHYLDOPA-CMC | METHYLDOPA-MAC | METHYLDOPA - HPC |
|----------------------------|------------|----------------------|----------------|----------------|------------------|
| E total (a.u) | -744.6087 | -1965.4083 | -2193.2291 | -2421.0934 | -2158.5677 |
| HOMO(ev) | -6.02608 | -5.84676 | -5.96186 | -5.99669 | -5.88912 |
| LUMO(ev) | -0.65468 | -0.22448 | -1.34829 | -1.00788 | -0.72598 |
| Eg(ΔE)ev | 5.37140 | 5.62227 | 4.61357 | 4.98881 | 5.16323 |
| IP (ev) | 6.02608 | 5.84676 | 5.96186 | 5.99669 | 5.88912 |
| EA(ev) | 0.65468 | 0.22448 | 1.34829 | 1.00788 | 0.72598 |
| χ (ev) | 3.34038 | 3.03562 | 3.65507 | 3.50228 | 3.30759 |
| μ (ev) | -3.34038 | -3.03562 | -3.65507 | -3.50228 | -3.30759 |
| η (ev ⁻¹) | 2.68570 | 2.81113 | 2.30678 | 2.49440 | 2.58161 |
| S (ev) | 0.37234 | 0.35572 | 0.43350 | 0.40089 | 0.38735 |
| GD (ev) | 2.07732 | 1.63901 | 2.89571 | 2.45870 | 2.11885 |
| D.M(debye) | 3.56128 | 4.032354 | 11.56338 | 18.35184 | 9.51831 |
| CP (ev) | -3.34038 | -3.03562 | -3.65507 | -3.50228 | -3.30759 |
| ΔN_{max} | 1.24376 | 1.07985 | 1.58448 | 1.40405 | 1.28121 |
| N(ev ⁻¹) | 0.48138 | 0.61012 | 0.34533 | 0.40671 | 0.47195 |

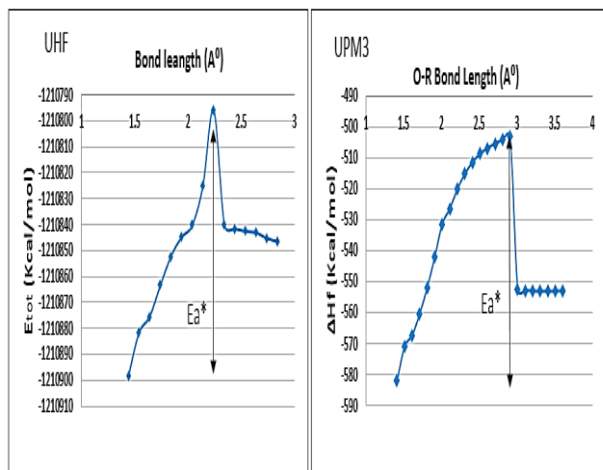


Fig. 5.1: Potential energy curve for O-R bond rupture in (methyl-dopa- cellulose)a using PM3 and U-HF method.

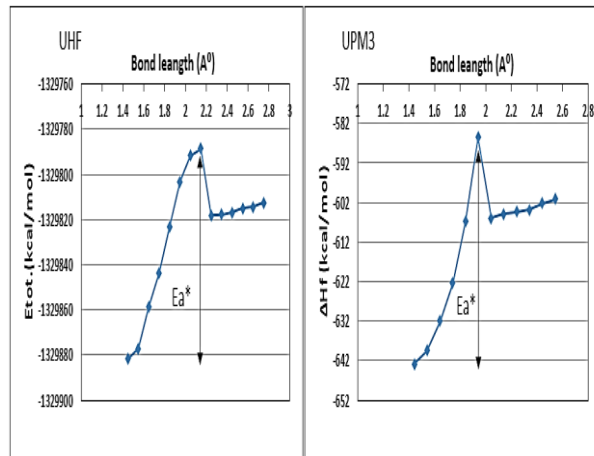


Fig.5.4: Potential energy curve for O-R bond rupture in (methyl-dopa- HPC) a using PM3 and U-HF method.

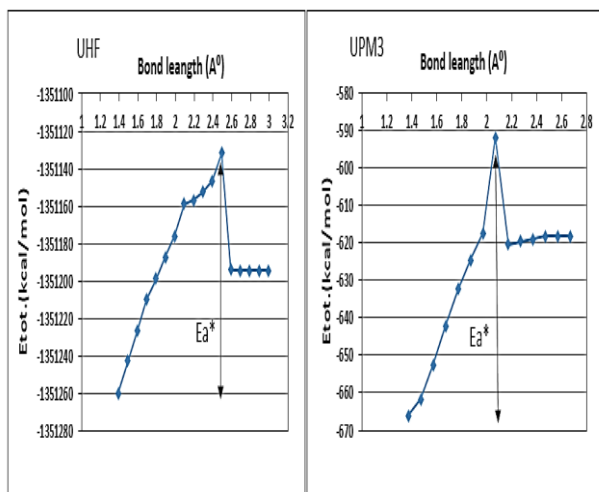


Fig. 5.2: Potential energy curve for O-R bond rupture in (methyl-dopa- CMC) a using PM3 and U-HF method.

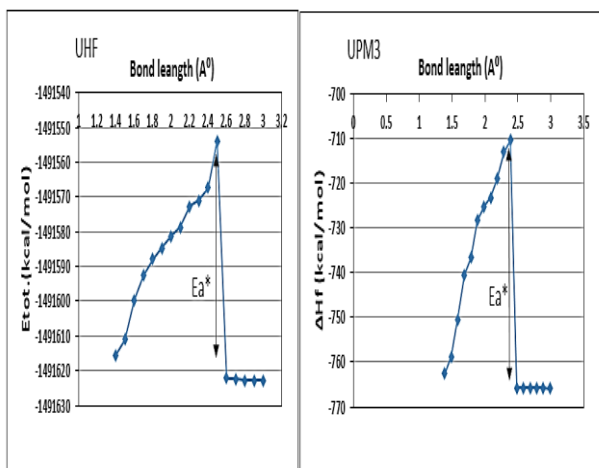


Fig.5.3: Potential energy curve for O-R bond rupture in (methyl-dopa- MAC) a using PM3 and U-HF method.

3.6. Predicted biological activity of prodrugs methyl-dopa:

Quantum chemical equations use the DFT method to determine compound biological activity. In aqueous medium the biological processes are normally done. The goal is to relate the biological activity of a number of methyl-dopa composition compounds to a number of descriptors in structure activity relationship studies. In several studies between different descriptors the electronic properties of molecules have been described by quantum chemical descriptors that are based on DFT[21]. Related parameters quantum chemical which are energy of the (EHOMO) [22], energy of the (ELUMO), energy gap (Egap), absolute softness (s), absolute electronegativity (c), chemical potential (CP), electrophilicity index (σ), nucleophilicity index (N), additional electronic charges (N) are all quantum chemical parameters that are linked (d,p). Table 5 lists these parameters.

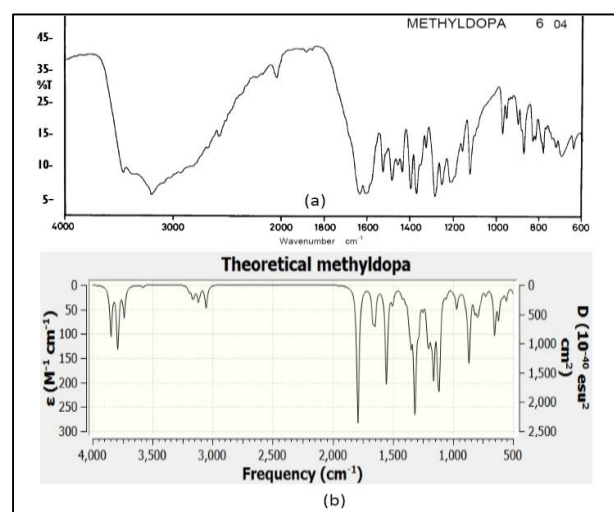


Fig. 9: IR spectrum for methyl-dopa a- experimentally b-theoretically by using DFT method.

In many chemical and pharmacological processes the energies of frontier molecular orbitals are important.

EHOMO measures the character of a compound's electron donation character, while ELUMO measures the character of its electron accepting character. For the active compound prodrug studied in this work, EHOMO is large (-5.846 eV) in methyl-dopa-cellulose, whereas the inactive compounds have low values. Hence, methyl-dopa is less efficient electron donor compounds than the inactive ones. The value energy ELUMO of the molecule is low, and this result shows that biological activity is increasing as ELUMO decreases, this means that the compounds (methyl-dopa and methyl-dopa-HPC) is more biological activity than the other compounds, as shown in the table (5). A biological structure is soft, such as a cell, enzyme, etc. Therefore, the biological reactivity of soft molecules is higher than that of hard molecules. Through the studied compounds, observed that the prodrug methyl-dopa-CMC is much softer (0.4335 eV). Low global electronegativity values or high chemical potential values mean that the electron is delocalized on the molecule so that the molecule can easily supply electrons to coordinate the proper structure. Therefore, (methyl-dopa-cellulose) is the lower value (3.0356 eV). Electrophilicity and nucleophilicity indices are the other parameters. According to them, biological reactivity in prodrugs (methyl-dopa-cellulose) increases with the nucleophilicity index and decreasing electrophilicity index [23], and lower nucleophilicity was observed in prodrugs (methyl-dopa-cellulose) (methyl-dopa-CMC).

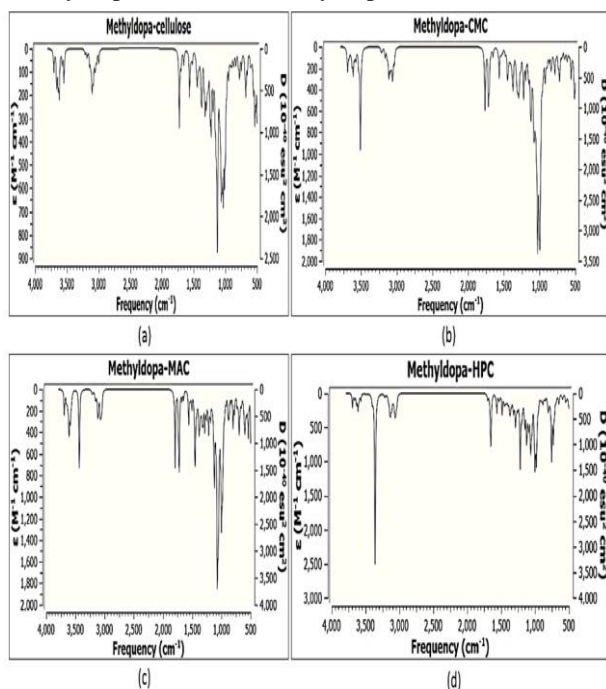


Fig.10: Calculated theoretical IR – Spectra of the a) methyl-dopa-cellulose, b) methyl-dopa-CMC, c) methyl-dopa-MAC, d) methyl-dopa-HPC.

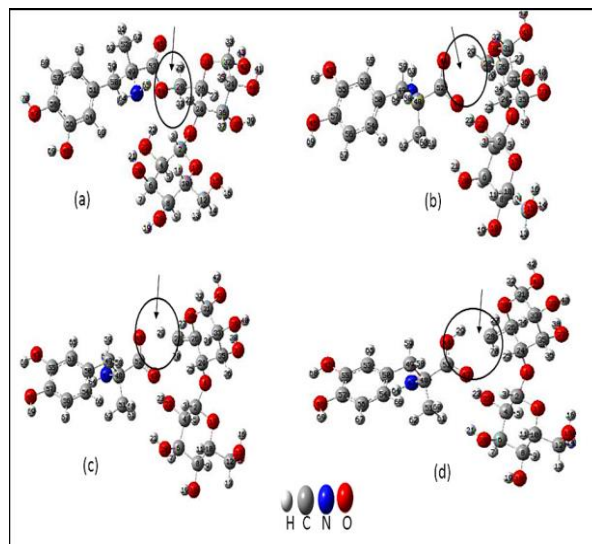


Fig.8.1: Geometrical structures for methyl-dopa (-cellulose) at: Equilibrium geometry (O-R= 1.44 Å), breakage bond (O...R= 1.54), Transition state (O..R= 2.24 Å), product at (2.34 Å).

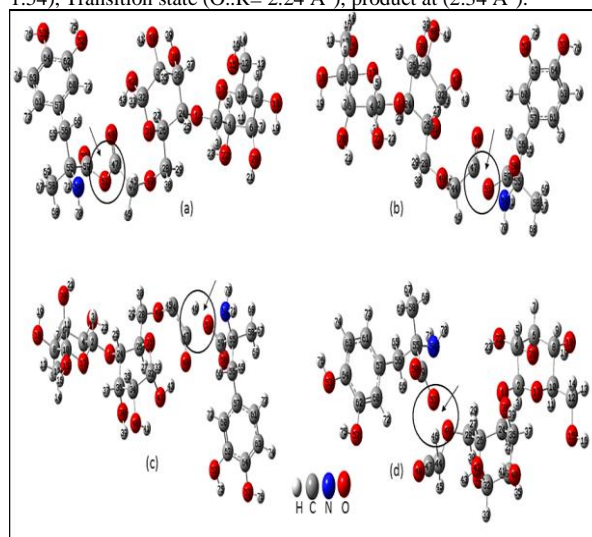


Fig. 8.2: Geometrical structures for (methyl-dopa-CMC) at: Equilibrium geometry (O-R= 1.39Å), breakage bond (O...R= 1.59), Transition state (O..R= 2.49 Å), product at (2.59 Å).

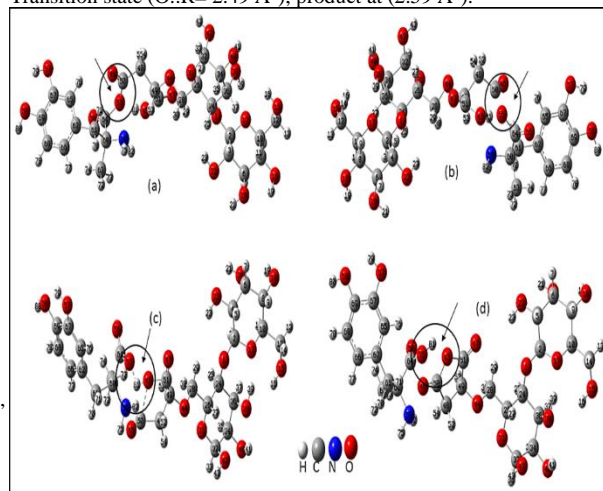


Fig.8.3: Geometrical structures for (methyl-dopa-MAC) at: Equilibrium geometry (O-R= 1.40Å), breakage bond (O...R= 1.50), Transition state (O..R= 2.50 Å), product at (2.60 Å).

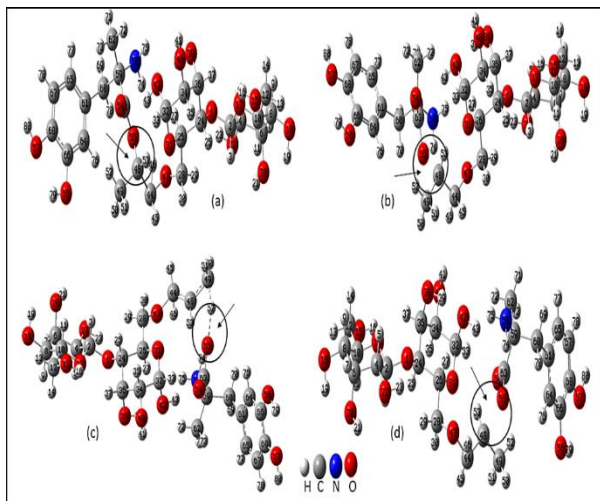


Fig.8.4: Geometrical structures for (methyl-dopa-HPC) at: Equilibrium geometry (O-R= 1.44 Å), breakage bond (O...R= 1.54 Å), Transition state (O..R= 2.14 Å), product at (2.24 Å).

4. Conclusions

The results of the calculation are considered as data we can call it as a new prodrug design are possible to test and synthesis it in the laboratory. The results of these studied prodrug the calculation led to obtaining the energies of the transition state, the products and the reactant. From the results that can obtained of determining for the best prodrug carriers. The methyl-dopa –CMC and HPC were not gave the acid drug and the low cracking heat (endothermic reaction) by using PM3 and U-HF/ STO-3G while activation energy for PM3and U-HF /STO-3G (74.11 to 57.25 kcal/mol) or from (127.94 to 93.13 kcal/mol), whilst Methyl-dopa –CE, Methyl-dopa –MAC , product acidic that in an irreversible reaction , Both ΔH_c and ΔE_c (endothermic reaction) 29.176 kcal/mol) and (52.136 kcal/mol) by PM3 and ab initio HF respectively, while prodrug (methyl-dopa-MAC) the cracking heat ΔH_c and ΔE_{tot} (cracking) was negative and exothermic (-3.256 and -7.243 kcal/mol methyl-dopa –CMC and methyl-dopa-CE, that be a good prodrug carrier according to relatively ΔH_c and ΔE_c kcal/mol and low activation energy. From the results in this study, biological activity high at an increasing highest occupied molecular orbital energy E_{HOMO} , electrophilic, chemical potential nucleophilic index, ΔN_{max} , and global softness with decreasing the electrophilicity. The important results was obtained is the decreasing of the energy gap and total energy that these molecules are more reactive than the original molecule.

5. Conflicts of interest

There are no conflicts to declare.

6. Acknowledgments

The authors would like to thank Mustansiriya University, College of Science, Chemistry Department, with their valuable contribution on these projects.

7. References

- [1] G. T. Mah, A. M. Tejani, and V. M. Musini, "Methyl-dopa for primary hypertension.," *Cochrane database Syst. Rev.*, vol. 2009, no. 4, p. CD003893, Oct. 2009, doi: 10.1002/14651858.CD003893.pub3.
- [2] S. Iliodromiti, F. Mackenzie, and R. S. Lindsay, "Methyl-dopa," *Pract. Diabetes Int.*, vol. 27, no. 4, pp. 166–167, 2010.
- [3] M. Thompson, "A Review of: 'Making Medicines—A Brief History of Pharmacy and Pharmaceuticals' Stuart Anderson, ed., ISBN# 0-85369-597-0, 318 pages, Hardcover, Pharmaceutical Press, Grayslake, IL, 2005." Taylor & Francis, 2006.
- [4] H. Kharkwal and S. Janaswamy, *Natural Polymers for Drug Delivery*. CABI, 2016.
- [5] B. Malhotra, H. Kharkwal, and M. P. Yadav, "2 Cellulose-based Polymeric Systems in Drug Delivery," *Nat. Polym. Drug Deliv.*, p. 10, 2016.
- [6] M. J. Frisch et al., "09, Revision D. 01, Gaussian," Inc., Wallingford, CT, 2009.
- [7] S. Wu, H. Yang, J. Hu, D. Shen, H. Zhang, and R. Xiao, "Pyrolysis of furan and its derivatives at 1100 C: PAH products and DFT study," *J. Anal. Appl. Pyrolysis*, vol. 120, pp. 252–257, 2016.
- [8] A. Sethi, R. P. Singh, and S. Gupta, "Synthesis of novel Steroidal-naproxen prodrugs, their molecular docking and theoretical studies by quantum chemical calculation.," *Chem. Biol. Interface*, vol. 8, no. 1, 2018.
- [9] M. L. Kadam, D. Patil, and N. Sekar, "Fluorescent carbazole based pyridone dyes—Synthesis, solvatochromism, linear and nonlinear optical properties," *Opt. Mater. (Amst.)*, vol. 85, pp. 308–318, 2018.
- [10] B. Mohan et al., "An experimental and computational study of pyrimidine based bis-uracil derivatives as efficient candidates for optical, nonlinear optical, and drug discovery applications," *Synth. Commun.*, vol. 50, no. 14, pp. 2199–2225, 2020.
- [11] M. U. Khan, M. Ibrahim, M. Khalid, S. Jamil, A. A. Al-Saadi, and M. R. S. A. Janjua, "Quantum chemical designing of indolo [3, 2, 1-jk] carbazole-based dyes for highly efficient nonlinear optical properties," *Chem. Phys. Lett.*, vol. 719, pp. 59–66, 2019.
- [12] Y. Yang, J. Liu, B. Zhang, and F. Liu, "Mechanistic studies of mercury adsorption and oxidation by oxygen over spinel-type $MnFe_2O_4$," *J. Hazard. Mater.*, vol. 321, pp. 154–161, 2017.
- [13] M. Belletête, J.-F. Morin, M. Leclerc, and G. Durocher, "A theoretical, spectroscopic, and photophysical study of 2, 7-carbazolevinylene-based conjugated derivatives," *J. Phys. Chem. A*, vol. 109, no. 31, pp. 6953–6959, 2005.
- [14] D. Zhenming, S. Heping, L. Yufang, L. Diansheng, and L. Bo, "Experimental and theoretical study of 10-methoxy-2-phenylbenzo [h] quinoline," *Spectrochim. Acta Part A Mol. Biomol. Spectrosc.*, vol. 78, no. 3, pp. 1143–1148, 2011.

- [15] R. Gupta, "Study of spectral and NLO properties of (2E)-1-(2,4-dihydroxyphenyl)-3-(4-hydroxyphenyl) prop-2-en-1-one by DFT," *Appl. Innov. Res.*, vol. 1, no. 3–4, pp. 160–170, 2020.
- [16] K. B. Benzon et al., "Spectroscopic, DFT, molecular dynamics and molecular docking study of 1-butyl-2-(4-hydroxyphenyl)-4,5-dimethyl-imidazole 3-oxide," *J. Mol. Struct.*, vol. 1134, pp. 330–344, 2017.
- [17] R. M. Kubba and A. A. Sallam, "Quantum mechanical calculations of RO thermal bond rupture energies in some ampicillin prodrugs," *Iraqi J. Sci.*, vol. 54, no. 4, pp. 739–752, 2013.
- [18] P. Verma, A. Verma, A. Namdev, and S. L. Soni, "Formulation and Evaluation of Gastroretentive Floating Tablets of Methyl Dopa," *Asian J. Pharm. Res. Dev.*, pp. 15–24, 2015.
- [19] V. Karunakaran and V. Balachandran, "Experimental and theoretical investigation of the molecular structure, conformational stability, hyperpolarizability, electrostatic potential, thermodynamic properties and NMR spectra of pharmaceutical important molecule: 4'-Methylpropiophenone," *Spectrochim. Acta Part A Mol. Biomol. Spectrosc.*, vol. 128, pp. 1–14, 2014.
- [20] J. Coates, "Interpretation of infrared spectra, a practical approach," *Encycl. Anal. Chem. Appl. theory Instrum.*, 2006.
- [21] A. M. Mansour, "Coordination behavior of sulfamethazine drug towards Ru (III) and Pt (II) ions: synthesis, spectral, DFT, magnetic, electrochemical and biological activity studies," *Inorganica Chim. Acta*, vol. 394, pp. 436–445, 2013.
- [22] K. Sayin, D. Karakaş, S. E. Kariper, and T. A. Sayin, "Computational study of some fluoroquinolones: Structural, spectral and docking investigations," *J. Mol. Struct.*, vol. 1156, pp. 172–181, 2018.
- [23] K. Sayin and D. Karakaş, "Investigation of Structural, Electronic and Biological Properties of Two Zn (II) Complexes with Pentaaza Macrocyclic Schiff-Base Ligand: A DFT Approach," *J. Clust. Sci.*, vol. 28, no. 6, pp. 3075–3086, 2017.